Determination of the effective refractive index of nanoparticulate ITO layers

M. Baum,[1,2,*] I. Alexeev,[1,2] M. Latzel,[3,4] S. H. Christiansen,[3,5] and M. Schmidt[1,2]

[1]*Institute of Photonic Technologies, Friedrich-Alexander-University Erlangen-Nuremberg, Paul-Gordan-Straße 3, 91052 Erlangen, Germany*
[2]*Erlangen Graduate School in Advanced Optical Technologies (SAOT), Friedrich-Alexander-University Erlangen Nuremberg, Paul-Gordan-Straße 6, 91052 Erlangen, Germany*
[3]*Max Planck Institute for the Science of Light, Günther-Scharowsky-Straße 1, 91058 Erlangen, Germany*
[4]*Institute of Optics, Information and Photonics, Friedrich-Alexander-University Erlangen-Nuremberg, Staudtstraße 7/B2, 91052 Erlangen, Germany*
[5]*Helmholtz Center Berlin, Hahn-Meitner Platz 1, 14109 Berlin, Germany*
[*]*marcus.baum@lpt.uni-erlangen.de*

Abstract: Nanoparticles of transparent conducting oxides, such as indium tin oxide, can be used in printing techniques to generate functional layers for various optoelectronic devices. Since these deposition methods do not create fully consolidated films, the optical properties of such layers are expected to be notably different from those of the bulk material and should be characterized on their own. In this work we present a way to measure the effective refractive index of a particulate ITO layer by refraction of light. The obtained data points are used to identify an accurate layer model for spectroscopic ellipsometry. In this way the complex refractive index of the particle layer is determined in a wide spectral range from ultra violet to near infrared.

©2013 Optical Society of America

OCIS codes: (310.6860) Thin films, optical properties; (050.1950) Diffraction gratings; (120.4530) Optical constants.

References and links

1. J. C. Manifacier, "Thin metallic oxides as transparent conductors," Thin Solid Films **90**(3), 297–308 (1982).
2. M. Groß, *Druckbare, nanopartikuläre Indiumzinnoxidschichten für optoelektronische Anwendungen*, Dissertation, Friedrich-Alexander-Universität Erlangen-Nuremberg, 2009, p.33.
3. T. Maruyama and K. Fukui, "Indium tin oxide thin films prepared by chemical vapour deposition," Thin Solid Films **203**(2), 297–302 (1991).
4. J. George and C. S. Menon, "Electrical and optical properties of electron beam evaporated ITO thin films," Surf. Coat. Tech. **132**(1), 45–48 (2000).
5. T. Minami, H. Sonohara, T. Kakumu, and S. Takata, "Physics of very thin ITO conducting films with high transparency prepared by DC magnetron sputtering," Thin Solid Films **270**(1-2), 37–42 (1995).
6. M. Baum, S. Polster, M. P. M. Jank, I. Alexeev, L. Frey, and M. Schmidt, "Efficient laser induced consolidation of nanoparticulate ZnO thin films with reduced thermal budget," Appl. Phys., A Mater. Sci. Process. **107**(2), 269–273 (2012).
7. M. Baum, H. Kim, I. Alexeev, A. Piqué, and M. Schmidt, "Generation of transparent conductive electrodes by laser consolidation of LIFT printed ITO nanoparticle layers," Appl. Phys., A Mater. Sci. Process. **111**(3), 799–805 (2013).
8. J.-S. Lee, M. V. Kovalenko, J. Huang, D. S. Chung, and D. V. Talapin, "Band-like transport, high electron mobility and high photoconductivity in all-inorganic nanocrystal arrays," Nat. Nanotechnol. **6**(6), 348–352 (2011).
9. S. Walther, S. Schäfer, M. P. M. Jank, H. Thiem, W. Peukert, L. Frey, and H. Ryssel, "Influence of annealing temperature and measurement ambient on TFTs based on gas phase synthesized ZnO nanoparticles," Microelectron. Eng. **87**(11), 2312–2316 (2010).
10. M. Hwang, B. Jeong, J. Moon, S.-K. Chun, and J. Kim, "Inkjekt-printing of indium tin oxide (ITO) films for transparent conducting electrodes," Mater. Sci. Eng. B **176**(14), 1128–1131 (2011).
11. D. A. G. Bruggeman, "Berechnung verschiedener physikalischer Konstanten von heterogenen Substanzen," Ann. Phys. **24**, 636–664 (1935).

#192282 - $15.00 USD Received 13 Jun 2013; revised 9 Aug 2013; accepted 19 Aug 2013; published 19 Sep 2013

12. H. Kim, C. M. Gilmore, A. Piqué, J. S. Horwitz, H. Mattoussi, H. Murata, Z. H. Kafafi, and D. B. Chrisey, "Electrical, optical, and structural properties of indium–tin–oxide thin films for organic light-emitting devices," J. Appl. Phys. **86**(11), 6451–6461 (1999).
13. I. Hamberg, C. G. Granqvist, K.-F. Berggren, B. E. Sernelius, and L. Engström, "Band-gap widening in heavily Sn-doped In2O3," Phys. Rev. B **30**, 3240–3249 (1984).
14. M. Baum, I. Alexeev, and M. Schmidt, "Laser Treatment of ITO and ZnO Nanoparticles for the Production of Thin Conducting Layers on Transparent Substrates," J. Laser Micro/Nanoeng. **6**(3), 191–194 (2011).
15. J. Ederth, P. Johnsson, G. A. Niklasson, A. Hoel, A. Hultaker, P. Heszler, C. G. Granqvist, A. R. van Doorn, M. J. Jongerius, and D. Burgard, "Electrical and optical properties of thin films consisting of tin-doped indium oxide nanoparticles," Phys. Rev. B **68**(15), 155410 (2003).
16. Eugene Hecht, *Optics. 4th Edition* (Addison Wesley Longman, Inc., USA, 2002).
17. M. Mahajeri, A. Schneider, M. Baum, T. Rechtenwald, M. Voigt, M. Schmidt, and W. Peukert, "Production of dispersions with small particle size from commercial indium tin oxide powder for the deposition of highly conductive and transparent films," Thin Solid Films **520**(17), 5741–5745 (2012).
18. A. Martínez, M. Sánchez-López, and I. Moreno, "Phasor analysis of binary diffraction gratings with different fill factors," Eur. J. Phys. **28**(5), 805–816 (2007).
19. M. Sánchez-López, I. Moreno, and A. Martínez-García, "Teaching diffraction gratings by means of a phasor analysis," Proc. SPIE ETOP (2009).
20. Y. Yang, X. W. Sun, B. J. Chen, C. X. Xu, T. P. Chen, C. Q. Sun, B. K. Tay, and Z. Sun, "Refractive indices of textured indium tin oxide and zinc oxide thin films," Thin Solid Films **510**(1-2), 95–101 (2006).
21. E. W. Tillotson, "The Relation of the Refractive Index of Soda Lime Glasses to Their Chemical Composition," J. Ind. Eng. Chem. **4**(4), 246–249 (1912).
22. H. A. Lorentz, *Encyclopädie der mathematischen Wissenschaften* (B.G. Teubner, 1904).</bok>

<jrn>23. P. Drude, "Zur Elektronentheorie der Metalle," Ann. Phys. **306**(3), 566–613 (1900).</jrn>

1. Introduction

Indium tin oxide (ITO) is a transparent semiconductor material commonly used in various optoelectronic devices such as solar cells, liquid crystal displays, touch-screens, and many others [1,2]. In these devices conductive ITO films are coated on the desired substrates by vacuum deposition methods [3–5]. Recently, alternative methods for ITO layer generation from nanoparticle suspensions have attracted considerable attention as a possible inexpensive alternative route for production of functional electronics [6–10]. If such materials are used for optoelectronic applications or laser processed, knowledge about their optical properties, especially their complex refractive index is needed. Since functional layers fabricated from nanoparticles tend to have residual porosity their optical properties are expected to be quite different from bulk material and must be investigated on their own.

Due to low accuracy in measurement or estimation of the porosity of thin nanoparticulate layers, effective medium theories like the often-cited Bruggeman theory [11] together with data for the bulk material cannot be used to gain accurate values of the film complex refractive index. Furthermore, the optical properties of bulk ITO depend on multiple factors, such as the composition i.e. content of tin-oxide and indium-oxide and the level of oxidization [12–15]. Thus, bulk material properties cannot be simply adopted from literature. Although there are a number of methods for determination of the material refractive index, they appear to be not well suited for the present case. Simplified approaches like estimating the layer absorption based on transmission curves and calculating the real part of the refractive index by Kramers-Kronig relations can provide only coarse estimations. As ITO is highly transparent in the visible wavelength region, accurate determination of the absorption is challenging. Furthermore the influences of the substrate as well as reflections and interferences have to be taken into account. The technique of attenuated total reflection spectroscopy (ATR), which is rather used for qualitative measurements, has deficits in the measurable range of refractive indices by nature, dependent on the material used to achieve total reflection. Moreover, in this method it is difficult to ensure optical contact between the sample layer and the ATR crystal.

Spectroscopic ellipsometry is commonly used for accurate determination of the complex refractive indices of thin films, but being an indirect measurement technique it requires an analytical model for the physical behavior and composition of the layered structure, which is not always known upfront. Furthermore, for porous layers the reflected light used for the

#192282 - $15.00 USD Received 13 Jun 2013; revised 9 Aug 2013; accepted 19 Aug 2013; published 19 Sep 2013
(C) 2013 OSA

measurement may deviate from the direct reflection by a comparable dense layer due to light scattering by particles within the layer [16].

In this paper we present results of experimental determination of the effective complex refractive index of ITO nanoparticle films obtained by combining diffraction analysis with spectroscopic ellipsometry. In the first step, the refractive index of an ITO film is determined for a finite set of light wavelengths using diffraction analysis. In the second step, the obtained values of n are used to identify an accurate layer model for ellipsometry data evaluation i.e. to remove ambiguity among the layer models that come into consideration.

2. Experimental details

2.1 Sample preparation

In our experiments, we used ITO nanoparticles with a particle size distribution ranging from 20 nm to 120 nm commercially available from Evonik Industries AG. We prepared an ITO suspension by dispersing the nanoparticles in ethanol at a 20 wt % loading. In order to prevent agglomeration of the particles in the suspensions we added 2-[2-(2-Methoxy-ethoxy)ethoxy]acetic acid, also known as trioxydecanoic acid, which works as a steric stabilizer. Details about the suspension preparation can be found in [17]. Then we generated ITO nanoparticle layers of uniform thickness on 25 mm x 25 mm x 1 mm soda-lime glass substrates by spin coating. Therefore, we deposited 200 µl of the suspension on the substrates and spun between 2600 rpm and 3000 rpm for 20 s. In order to determine the film thickness we introduced scratches on the sample surface and measured several height profiles of these structures with a laser scanning microscope (Olympus Lext OLS4000). We performed these height measurements for each analyzed sample. For the measurement of the optical transmission properties of the layers we used an UV-Vis spectrometer (Shimadzu, UV-3600).

2.2 Determination of the refractive index by diffraction

In order to determine the refractive index of the nanoparticulate ITO layers we fabricated transmission gratings by partly ablating the deposited particle films with an ultrafast laser (Time Bandwidth Fuego, 1064 nm central wavelength, 10 ps pulse duration). The target structure is shown in Fig. 1(a). For this experiment we used ITO layers produced at a spinning rate of 2700 rpm with a resulting film thickness of 740 nm ± 20 nm. We placed the coated glass plates in the focal plane of the structuring laser beam (30 µm in diameter), and scanned the beam over the sample surface in a linear raster pattern. We kept the scanning speed constant at 50 mm/s with a pulse repetition rate of 200 kHz. In order to tune the diameter of the circular ablations, we adjusted the laser power keeping it below 3 W where the ablation threshold for the glass substrates is reached. To achieve circular ablations with a diameter of 25 µm, we used a laser power of 1.30 W. With a line separation of 50 µm we produced a grating structure with a period of 50 µm (50% fill factor) and a spatial dimension of 15 mm x 20 mm. Figure 1(b) shows a 3D image of the fabricated ITO grating. We used low intensity collimated beams of different diode lasers with wavelengths of 405 nm, 632 nm and 980 nm as well as a frequency doubled Nd:YAG laser at 532 nm to illuminate the grating from the glass side at normal incidence. For each wavelength, we recorded the diffraction pattern produced by the grating by a CCD camera (UI-2140SE from IDS Imaging) which was moved on a rail perpendicular to the incident nondiffracted laser beam at a distance of 4 m away from the grating. Since the dynamic range of the 8 bit camera was not sufficient to cover the full range of occurring intensities, we equalized the peak intensities of the diffraction orders by introducing calibrated neutral density filters into the beam path.

#192282 - $15.00 USD Received 13 Jun 2013; revised 9 Aug 2013; accepted 19 Aug 2013; published 19 Sep 2013
(C) 2013 OSA

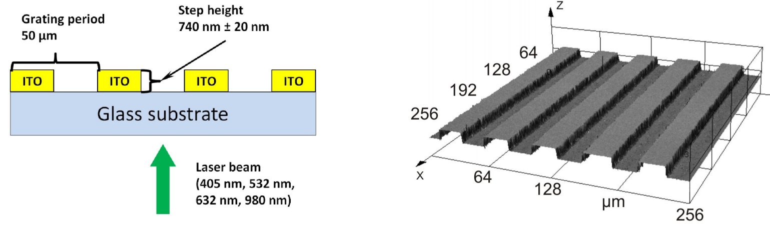

Fig. 1. (a) Schematic diagram of the transmission grating. (b) LSM image of the fabricated diffraction grating with step height of 740 nm ± 20 nm, diffraction period of 50 µm and 50% fill factor.

2.3 Analysis of the diffraction pattern

If the transparent structure shown in Fig. 1 is irradiated with a collimated light beam, it will diffract the light into multiple diffraction orders according to the well-established diffraction theory. The deflection angles can be calculated from the diffraction grating law and will depend on the wavelength of the incident light and the grating period, while the relative intensity of the diffracted orders will be affected by the grating fill factor and the phase shift introduced by the imposed ITO structure. Extending the phasor analysis presented in [18,19], the intensity of the mth diffraction order can be calculated as $I_m = |G_m|^2$ where the amplitude G_m is expressed as:

$$G_m = \frac{1}{p}\int_{-p/2}^{p/2} \mathrm{g}(x)\exp\left(im\frac{2\pi x}{p}\right)dx \tag{1}$$

Here, p is the diffraction period with the transmittance profile g(x) given by:

$$\mathrm{g}(x) = \begin{cases} Ae^{i\varphi} & \text{if } x \in [-p/2, -p/2 + ap] \\ 1 & \text{if } x \in [-p/2 + ap, +p/2] \end{cases} \tag{2}$$

In this calculation, A^2 is the relative amplitude of the light intensities transmitted through the coated and bare glass regions of the grating, $\varphi = 2\pi L(n_\lambda - 1)/\lambda$ is the phase shift introduced by the grating structure for normal incidence. It contains the primary information about the ITO layer refractive index. L and λ are the grating profile height and light wavelength respectively. In case of $a = 0.5$ corresponding to a grating fill factor of 50%, I_m reduces to:

$$I_m = \begin{cases} \left[(1-A)^2 + 4A\sin^2\left(\frac{\varphi}{2}\right)\right]\cdot\frac{\sin^2(0.5m\pi)}{m^2\pi^2} & \text{for } m = 1,2,3... \\ \frac{1}{4}\left[(1-A)^2 + 4A\cos^2\left(\frac{\varphi}{2}\right)\right] & \text{for } m = 0 \end{cases} \tag{3}$$

The relative light transmission A^2 through the air – glass and air – ITO – glass interfaces, that can be evaluated based on Fresnel's equations, also depends on the ITO layer refractive index. Although the latter is not known, the possible variation of A can easily be estimated by assuming that the typical refractive index of a dense, sputtered ITO layer of about 2.2 at 400 nm [20] represents an upper boundary for the layer refractive index resulting in $1 < n_{ITOlayer} < 2.2$. The refractive index of soda-lime glass ranges from 1.5 to 1.6 depending on its chemical composition [21], which leads to $0.93 < \mathrm{A} < 1$. This holds true in the wavelength region between 400 nm and 1000 nm where the imaginary part of the refractive index should be close to zero according to transmission curves shown in Fig. 4. Based on

#192282 - $15.00 USD Received 13 Jun 2013; revised 9 Aug 2013; accepted 19 Aug 2013; published 19 Sep 2013
(C) 2013 OSA

those measurements absorption in the ITO film was estimated to be below 4% for the spectral range specified above. For a relatively porous ITO layer the effective refractive index is expected to be in the vicinity of the mid value ($n_{ITO\ layer}$ ~1.6) being quite close to the refractive index of the glass substrate and effectively making the term $(1\text{-}A)^2$ negligibly small. Thus, formula (3) simplifies further to:

$$I_m = \begin{cases} \frac{4}{m^2\pi^2}\sin^2\left(\frac{\varphi}{2}\right)\cdot\sin^2\left(\frac{m\pi}{2}\right) & for\, m = 1,2,3... \\ \cos^2\left(\frac{\varphi}{2}\right) & for\, m = 0 \end{cases} \tag{4}$$

Since only the relative amplitude of the diffraction orders is of interest the linear dependence of I_m on A was omitted as it occurs for all m. By measuring the relative peak intensity of the diffraction orders and fitting the experimental data with formula (4), the grating induced phase shift can be determined allowing the deduction of the layer effective refractive index. Figure 2 shows the experimentally measured diffraction order intensity distribution normalized with respect to the highest occurring intensity as well as the fitted values for a single wavelength (632 nm), while data for the other wavelengths is omitted for picture clarity. Although, there is some ambiguity in determination of the phase shift φ due to the periodicity and symmetry of $\sin^2$ function, it can be removed by physical considerations. The acceptable values of the refractive index are expected to be in the range $1 < n < n_{sputtered}$ due to layer porosity and consistency with the Clausius-Mossotti equation and they shall show normal monotonical dispersion behavior as well. After elimination of the nonphysical results the values consistent with the above specified criteria are presented in Table 1. The given errors are calculated based on the accuracy in the measurement of the layer thickness. The values are compared later on with values obtained by spectroscopic ellipsometry in order to identify an accurate model for the physical behavior of the nanoparticulate layer.

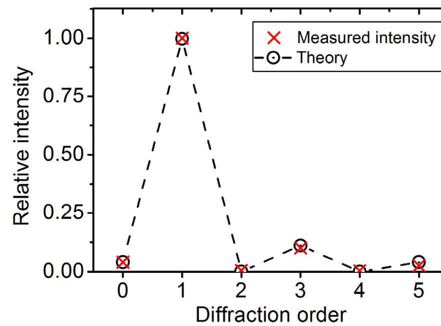

Fig. 2. Relative intensity of the diffraction orders recorded for the 632 nm laser normalized with respect to the highest occurring intensity (red crosses) and the fitted values predicted by the theory (black circles). The lines are a guide to the eye only.

Table 1. Nanoparticle ITO Layer Index of Refraction

Wavelength, nm	405	532	633	980
n	1.526 ± 0.015	1.500 ± 0.014	1.462 ± 0.012	1.360 ± 0.010

2.4 Determination of the complex refractive index based on ellipsometry

We took ellipsometric spectra of a particle layer prepared by spin coating at 3000 rpm with a thickness of 540 nm ± 20 nm on a soda-lime substrate as well as spectra of an uncoated substrate using the above-mentioned spectroscopic ellipsometer (UVISEL, Horiba Jobin Yvon). The spectra were taken in the wavelength range between 190 nm and 2000 nm, while

#192282 - $15.00 USD Received 13 Jun 2013; revised 9 Aug 2013; accepted 19 Aug 2013; published 19 Sep 2013
(C) 2013 OSA

the angle of incidence was kept constant at 70°. The modulator and analyzer of the ellipsometer were fixed at 0° and 45°, respectively so that the Mueller matrix elements I_s and I_c are given by:

$$I_S = \sin 2\Psi \times \sin\Delta \\ I_C = \sin 2\Psi \times \cos\Delta \quad (5)$$

Here Ψ and Δ denote the ellipsometric parameters. It is worth mentioning that due to scattering of light by the particles polarization is likely to not be fully conserved especially for short wavelengths. As a consequence fitting of an appropriate model for the layer is impeded resulting in a certain ambiguity in the choice of models.

We benchmarked the models used for ellipsometric analysis based on the merit function χ^2 between the experimental and predicted data for I_c and I_s. The merit function should be minimal and is given by:

$$\chi^2 = \frac{1}{2N-P-1}\sum_{i=1}^{N}\left[\left(\frac{I_{s-m_i} - I_{s-c_i}(\lambda_i)}{\sigma_{s-m_i}}\right)^2 + \left(\frac{I_{c-m_i} - I_{c-c_i}(\lambda_i)}{\sigma_{c-m_i}}\right)^2\right] \quad (6)$$

Here, N and P denote the number of experimental data points and the number of parameters modeling the sample. $I_{s\text{-}mi}$ and $I_{c\text{-}mi}$ are the measured quantities at wavelength λ_i while $I_{s\text{-}ci}$ and $I_{c\text{-}ci}$ are the corresponding quantities calculated by the model used. $\sigma_{s\text{-}mi}$ and $\sigma_{c\text{-}mi}$ are the associated experimental errors. The software used for data evaluation was DeltaPsi2 by Horiba Jobin Yvon provided with the ellipsometer.

In order to obtain the optical properties of the soda-lime glass substrates we measured the spectrum of an uncoated glass piece. Its dielectric function was modeled by a Lorentzian oscillator and treated as being infinitely thick. This model fits excellently, which becomes apparent in a value of χ^2 as low as 0.03. For modeling the particle layer, besides minimizing the merit function χ^2 in the range from 300 nm to 1500 nm also the obtained values for n resulting from the particular model were compared with the values for n measured by evaluation of the grating diffraction presented above. The setup used to model the particle layer behavior which best matches these values while at the same time possessing a minimal merit function was a planar soda-lime substrate of infinite thickness with the previously determined optical properties and a dense coating with an unknown thickness. We modeled the optical behavior of the coating by a single Lorentzian oscillator in combination with Drude absorption representing the band gap and the presence of free electrons, respectively. The corresponding dielectric function is given by [22,23]:

$$\varepsilon = \varepsilon_\infty + \frac{(\varepsilon_s - \varepsilon_\infty)\omega_t^2}{\omega_t^2 - \omega^2 + i\Gamma_0\omega} + \frac{\omega_p^2}{-\omega^2 + i\Gamma_D\omega} \quad (7)$$

Where ω_t and ω_p are the the resonance frequencies of the bandgap and the plasma edge, respectively and $\Gamma_{0/D}$ denote the corresponding damping factors. All of these variables as well as the layer thickness were used as fitting parameters.

#192282 - $15.00 USD Received 13 Jun 2013; revised 9 Aug 2013; accepted 19 Aug 2013; published 19 Sep 2013
(C) 2013 OSA

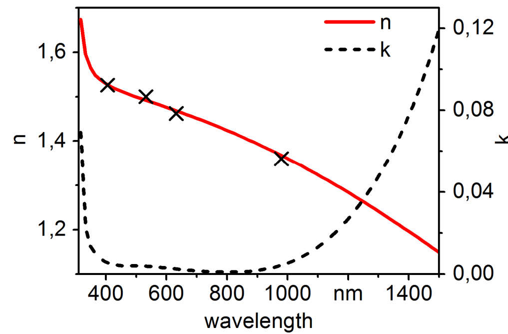

Fig. 3. Effective refractive index of the ITO layer given by the chosen ellipsometric model. The black crosses mark the values of n determined by diffraction pattern evaluation.

While the value of the merit function χ^2 of 7.56 appears to be relatively high for the chosen model, the values for n determined by evaluation of the diffraction patterns match very well to the curve given by the model (see Fig. 3). At the same time the layer thickness was determined to be 558.6 nm ± 4.3 nm by the fit which is in good agreement with the expected layer thickness.

3. Validation of the obtained results by simulation

In order to validate the obtained results for the layer refractive index by an independent method, we carried out simulations in FDTD solutions 8.5.1. by Lumerical Solutions, Inc. Here, the particle layer was modeled as a two dimensional slab placed on a soda-lime substrate. A continuous light source was applied pointing towards the slab surface perpendicularly. For the effective refractive index of the slab we used the data for *n* and *k* given by the ellipsometer measurement. The result of the simulation are shown in Fig. 4 for an exemplary simulation of an ITO slab with a thickness of 800 nm in comparison with the experimentally acquired transmission of an actual particle layer with a thickness of 800 nm ± 20 nm on a soda-lime substrate. The larger sample thickness shown was chosen due to its more pronounced decay in transmission for longer wavelengths in comparison to thinner layers. Further simulations for different layer thicknesses (not shown here) are also in good agreement with the corresponding measurements.

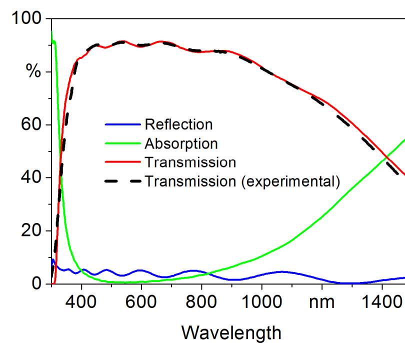

Fig. 4. Transmission, absorption and reflection (direct + diffuse) calculated in the simulation as well as the measured transmission for a particle layer with a thickness of 800 nm (dashed line)

4. Conclusion

In this work we proposed a way of determining the effective complex refractive index of a porous ITO layer. Discrete values of the refractive index have been measured by evaluation

#192282 - $15.00 USD Received 13 Jun 2013; revised 9 Aug 2013; accepted 19 Aug 2013; published 19 Sep 2013
(C) 2013 OSA

of refraction patterns produced by gratings of the considered material. Here the values of the real part of the refractive index can be found easily by a simple and unique formula. This approach works for wavelengths where the layer has close to zero absorption. The obtained values were used to identify an appropriate layer model for spectroscopic ellipsometry. In this way a data set of refractive indices over the whole wavelength region from 300 nm to 1500 nm was obtained without requiring information about the actual layer porosity. However, equal porosity has to be assumed for all particle layers. Simulations of the transmission of thin layers were in excellent agreement with experimentally determined transmission curves confirming the accuracy of the measurement.

Acknowledgments

The support of the German Research Foundation (DFG, Graduiertenkolleg 1161/2) is gratefully acknowledged. Additionally, we are thankful for the support by Evonik Industries AG. Moreover, the authors gratefully acknowledge funding of the Erlangen Graduate School in Advanced Optical Technologies (SAOT) by the German Research Foundation (DFG) in the framework of the German excellence initiative as well as the support of the Cluster of Excellence for Engineering of Advanced Materials (EAM). Furthermore, we acknowledge support by Deutsche Forschungsgemeinschaft and Friedrich-Alexander-Universität Erlangen-Nürnberg within the funding programme Open Access Publishing.